POLITECNICO
MILANO 1863

DIPARTIMENTO DI MECCANICA

mecc

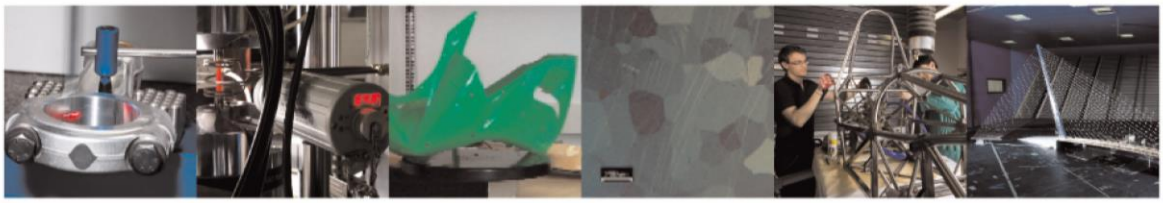

Energy oriented multi cutting parameter optimization in face milling

ALBERTELLI, PAOLO; KESHARI, ANUPAM; MATTA, ANDREA

This is a post-peer-review, pre-copyedit version of an article published in JOURNAL OF CLEANER PRODUCTION. The final authenticated version is available online at: http://dx.doi.org/10.1016/j.jclepro.2016.04.012

This content is provided under CC BY-NC-ND 4.0 license

DIPARTIMENTO DI MECCANICA ■ POLITECNICO DI MILANO
via G. La Masa, 1 ■ 20156 Milano ■ EMAIL (PEC): pecmecc@cert.polimi.it
http://www.mecc.polimi.it
Rev. 0

Wordcount for the whole text file: 10532

Energy oriented multi cutting parameter optimization in face milling

Paolo Albertelli[a*], Anupam Keshari[a,b], Andrea Matta[c]

[a]*Department of Mechanical Engineering, Politecnico di Milano, Milan, Italy.*

[b]*Laboratory of Machine Tools and Production Systems, Consorzio MUSP, Piacenza, Italy.*

[c] *Department of Industrial Engineering and Management, Jiao Tong University, Shanghai, China.*

* Corresponding author. *E-mail address:* paolo.albertelli@polimi.it

Abstract

A new model for evaluating the energy consumed by a machine tool for processing a prismatic workpiece was developed. The model takes into account the energy absorbed by different machine components such as the auxiliary systems, the axes, the axes chiller, the tool change system, chip conveyor and the spindle system. The relationships between the power absorption of each considered machine component and the main cutting parameters were adequately modelled. The cutting energy was also taken into consideration. Since the wear of the tool was included in the model, the energy absorbed by the machine during passive phases (e.g. tool changes) was also evaluated. Each machine component model was opportunely configured according to the considered production phase. Some of the parameters of the machine tool energy model were identified through experimental tests performed on a real machining center equipped with linear motors. A multivariable energy optimization was carried out considering the cutting speed, the feed and the radial depth of cut as the main parameters. The energy minimization was performed through exhaustive enumeration methods. Results were properly discussed and analyzed. The optimization analysis was also repeated emulating various machine tool configurations and different production scenarios.

Keywords: Machine Tool Energy modelling; Multi-parameter energy Optimization; Energy Saving

1. Introduction

Manufacturing is one of the most energy demanding industrial sectors, thus many potential energy saving opportunities can be conceived, analyzed and tested. Universities and research centers, together with industries, are dealing with this topic. Since machine tools are highly widespread in production systems, many research efforts have been focusing on their energy consumption reduction (Diaz et al. (2010a), Diaz et al. (2010b)). Energy savings in machine tools can be achieved by a proper energy-oriented machine tool components design or by a better machine usage, both in terms of machining strategy and process parameter selection, Diaz et al. (2009) and Yingjie (2014).

The awareness of machine tool energy consumption during its use is the key point for conceiving further energy saving solutions. Consequently, a detailed and comprehensive energy assessment is surely needed. The experimental approach is one of the methodologies that can be used to perform a machine tool energy evaluation (e.g. Behrendt et al. (2012)) even if it presents some limiting aspects. In fact, the experimental procedure is costly and time consuming, especially if the machine tool energy characterization has to be performed in many process conditions and for different machining strategies. Moreover, if the power assessment needs to be performed at machine tool component level, a complex and expensive instrumentation able to simultaneously monitor several machine tool functional modules (e.g. machine axes, chillers and cooling systems, spindle, process cooling systems, etc.) is requested. As a consequence, the availability of reliable energy models able to overcome the above described limitations is becoming essential. Machine tool energy models can be used for disparate purposes. In fact, they can be very useful for predicting the consumed energy in different working conditions or when different

machining parameters are adopted. They can even be used for testing both various machine tool configurations and energy oriented design improvements (i.e. Huang and Ameta (2014)).

According to Schmidt et al. (2015), different energy modelling approaches have been conceived in manufacturing. Some researchers used the Exergy concept to evaluate the maximum useful work linked to a specific manufacturing process. For instance, Gutowski et al. (2006) adopted this approach to analyze several manufacturing processes. In particular, they have found a theoretical reverse trend between specific energy consumption (SEC – energy per unit of processed material) and the process rate. This approach cannot be easily applied to machine tools because the coefficients of the theoretical relationship are generally missing. Thiede et al. (2012) proposed a quick and easy energy consumption estimation method based on nominal power data from type plates or machine specifications. In a similar way, He et al. (2012) proposed an approach to estimate the energy consumption of a machine tool or a lathe starting from the NC code. The approaches are not particularly suitable for complex machine tools and they involve too high estimating errors. Due to the described limitations, approaches based on empirical energy models are typically preferred. Even if improvements can be still accomplished (Zhou et al (2015)), the combination of experimental and analytical procedures seems to be the more profitable way to tackle the machine tool energy consumption estimation.

For instance, Diaz et al. (2009) proposed a simple direct modelling approach where it is assumed that the total energy absorption can be computed using the following equation:

$$\text{Total energy consumption} = (P_{air} + P_{cut}) \cdot \Delta t = (P_{air} + MRR \cdot SCE) \cdot \Delta t$$

where, P_{cut} is the power used by spindle to remove the material, P_{air} is the power used by the machine when operations are performed in air and Δt is the processing time. The cutting power P_{cut} depends on MRR (Material Removal Rate) and on the SCE (Specific Cutting Energy) that is generally identified by means of experiments. Since the proposed models show that the overall consumed energy depends on SCE and on the volume of processed material, a specific study focused on the effects of each process parameter cannot be carried out. This is mainly due to a lack of details in the energy models. Similar simple models that involve SCE and MRR were formulated by Li and Kara (2011) and Kara and Li (2011). Hu et al. (2012) developed an on-line approach for monitoring the machine tool efficiency. The approach was based on a simple model that had been characterized through experiments. Newman et al. (2012) worked on a theoretical framework for creating a machine tool energy model. The authors also proposed a reference workpiece that can be used to perform a machine tool experimental energy assessment. Gotze et al. (2012) proposed an energy-oriented methodology for evaluating machine tools and modelling the energy flows. The approach was also used to outline economic considerations. The author analyzed mainly the machine drives focusing on the estimation of the energy saving potentials of the braking energy storage systems. Balogun and Mativenga (2013) presented an energy model by decomposing the power consumption in terms of basic power, “ready state” power, coolant pumping power and the power used by the machine during air cutting. In order to compute the energy, total processing time was divided into time spend in basic state, time spend in ready state, time spend for tool movement in air and cutting time. The modeling was based on experimental energy measurements. Li et al. (2013) presented an empirical model for the evaluation of the absorbed energy in face milling operations. In order to predict the energy consumption in the spindle system, experimental tests were carried out to estimate the specific cutting energy and the spindle power consumption. The model considers the global energy as a function of both the MRR and the spindle speed. Yang et al. (2013) proposed a method to create an energy machine tool model through GRASP (Greedy Randomized Adaptive Search Procedure) approach. Draganescu et al. (2003), focusing mainly on the machining phase, created a model for estimating both the machine tool efficiency and the specific energy consumption. The model was specifically developed for a vertical-milling machine. The study of the influence of the main cutting parameters (feed rate, axial depth of cut, radial depth of cut, cutting speed and number of teeth) was carried out. Since the majority of the analyzed modelling approaches are based on empirical relationships that consider the machine tool as a whole, the energy contribution of each single machine tool functional module cannot be distinguished. The observed limitation can be particularly detrimental when it is necessary to deeply analyze and compare energy saving strategies. Indeed, the power consumption of each single machine center component usually depends on process parameters.

Over the years, many researchers focused on machining parameter selection but only a few recent researches have dealt with energy consumption issues. For instance, Diaz et al. (2009) made a review of the machine tool energy consumption reduction policies. Mori et al. (2011) presented a study on the effects of cutting parameters on total energy consumptions in face-milling operations: axial and radial depths of cut, feed rate and cutting speed were identified as the main cutting parameters. Rajemi et al. (2010) and Mativenga and Rajemi (2011) performed an energy minimization through a proper cutting speed selection in turning taking into consideration the tool wear. The total energy consumption was estimated using an empirical energy model that considers the energy absorption during workpiece setup, machining and tool changes. The analysis of the effect of considering the tool energy footprint in the minimization procedure was also performed. Balogun et al. (2013) dealt with the minimization of energy consumption in turning and other machining operations. Li et al. (2014) presented an energy consumption analytical model for CNC machine tools. The authors performed a multi-objective (energy and production time) optimization through a proper selection of the main cutting parameters. Genetic algorithms were adopted for the optimization. The proposed approach does not allow getting a clear understanding of the energy consumed in the main functional modules and in which way the process parameters affect the overall absorbed energy. Moreover, the developed model does not consider both the tool wear and the machining strategies. Wang et al. (2014) presented a multi-objective cutting parameter optimization. The energy consumption, the production costs and the workpiece quality were simultaneously considered in the presented analysis. Feed rate, depth of cut and cutting speed were the optimized cutting parameters. The cutting strategy was not included in the energy model used in the optimization. Hanafi et al. (2012) dealt with a multi-objective turning optimization that was focused both on the energy footprint and on the piece quality. An experimental approach that involved several tests was adopted: cutting power and surface roughness were recorded for each test condition while cutting speed, feed and depth of cut were the analyzed parameters. A response surface model, which interpolates locally the response functions, was developed. The majority of the analyzed researches gave much attention to the adopted optimization techniques instead of understanding the effects of the cutting parameter selection and what are the energy contributions of different machine tool functional modules.

1.1. Research aim and scope

This research deals with multi-cutting parameter energy oriented optimization of milling operations. In order to overcome the limitations of the analyzed literature on energy models, a detailed and holistic analytical model of the energy absorbed by a CNC machine center was developed. No previous works that proposed such a holistic approach in machine tool energy modelling and multi-parameter optimization have been found. Since the model is quite complex, the results of the optimization could not have been easily predicted. The enhanced energy model was developed in order to fulfill all the requirements needed to perform a multi-variable optimization. To achieve this goal, the dependence on the main cutting parameters was modelled. For each considered machine tool functional module, a configurable energy model was proposed. In fact, each energy sub-system model can be set according to the specific task the machine is doing. The developed model takes into account the tool wear and all the machine movements that need to be executed to change the tool. Such a model is also suitable for comparing different machining strategies. In reality, during the machining strategy definition, many technological choices (e.g. a proper selection of the number of passes, the tool-workpiece engagement and the workpiece approaching strategy, the feed direction and the cutting velocity) must be carried out. Consequently, a model able to evaluate all the energy implications connected to the performed choices would be very useful.

In order to accomplish this goal, machine tool axes and face milling process were adequately modelled. For instance, the energy absorbed by the axes does not depend only on the feed velocity but also on the axis load (due to the action of the cutting forces) and consequently it depends on all the main cutting parameters. An analytical formulation for the axis load computation was proposed starting from a well-known literature mechanistic cutting process model, Altintas (2012). Some of the parameters of the energy model were identified analyzing experimental tests performed on a CNC machine with a horizontal spindle and equipped with linear motors. Focusing on a prismatic workpiece processing, the developed model was used to find out the cutting condition that minimizes the overall energy consumption (Specific Energy) through a multi-dimensional exhaustive enumeration method. The considered process parameters were evaluated within their feasible technological ranges.

Considerations about the obtained results, especially comparing with those obtained from the production time minimization, were made. Different processed materials were also analyzed. Moreover, a sensitive analysis changing some model parameters was made fictitiously simulating both different production scenarios and different machines. The schematic representation of the adopted modelling approach is reported in Fig. 1.

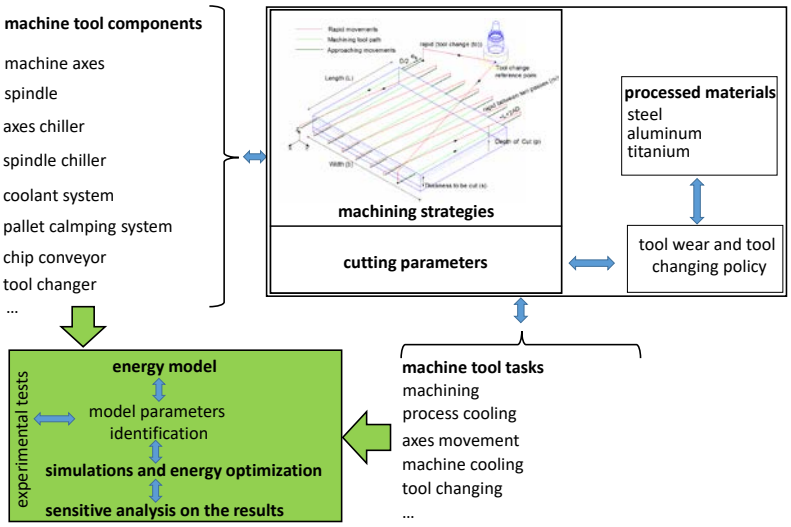

Fig. 1: schematic representation of the proposed energy modelling approach

The paper is structured as follows. The description of the developed energy model is reported in section 2. The experimental procedure used to update the model parameters is described in section 3. Discussion on the results coming from the cutting condition optimization considering separately both the minimization of the global energy and the production time is reported in section 4. Other simulation results considering different scenarios are reported in section 5. Conclusions and possible future outcomes are presented in section 6.

2. Analytical model to estimate energy consumption in face milling operation

In this paper section, both the description of the considered technological scenario and the details of the developed analytical models will be presented. As a technological reference case Fig. 2, we considered a generic prismatic workpiece, processed through face milling operations. In Fig. 2, the analyzed cutting strategy is also reported. In order to prevent any dependence on the workpiece dimensions, the developed models (both for production time and for the consumed energy) refer to the unit of the processed material volume.

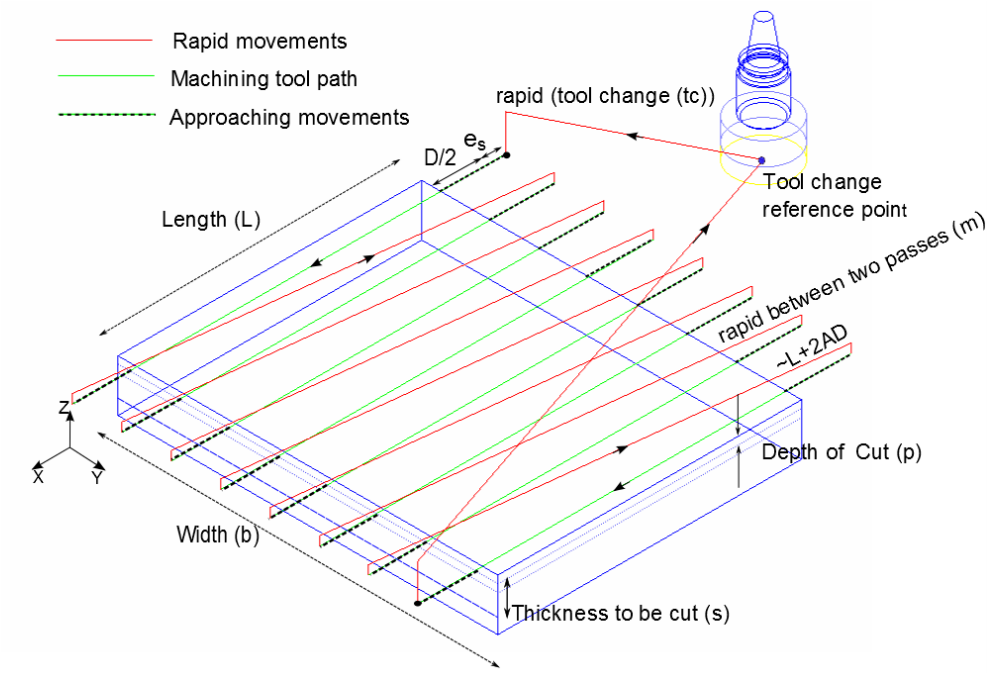

Fig. 2: Selected machining strategy based on face milling operations (machine tool tasks)

The energy model was developed starting from a preliminary version presented in Albertelli et al. (2011) and in Calvanese et al. (2013). The here developed model is able to evaluate the machine tool power consumption (detailing the contributions of its main components) in different production phases (i.e. machining, tool change, workpiece preparation) and even when different cutting parameters values (radial depth of cut, feed and cutting speed) are selected. For doing that, all the considered machine tool functional modules were adequately modelled according to the specific considered production phase. In fact, the energy model can be opportunely set on the base the specific machine tasks. For instance, the developed axes model was configured for the machining phase, the workpiece approaching, the tool changes and the machine rapid positioning. Some of the axis energy model configurations take into account the dependence on the main cutting parameters. For other machine tool components, energy models have a reduced number of configurations. For example, the chip conveyor system shows a simpler energy model that does not depend on the main cutting parameters. Some of the adopted assumptions are aligned with Avram and Xirouchakis (2011). Additional hypotheses will be progressively introduced in this paper section.

Since the energy is defined as the integral of power over time, the power consumption model of each considered machine functional module together with the durations of different production phases need to be defined.

2.1. Production phases definition

In this subsection, a detailed description of the production phases is reported. The overall task duration depends on the process parameters.

The whole processing time (t) is composed by the following contributions, Eq. (1):

$$t = t_1 + t_2 + t_3 \quad (1)$$

Where t_1 represents the time required to execute the workpiece setup; t_2 the machining time while t_3 accounts for all the time intervals in which the tool is not engaged in the workpiece.

According to Eq. (2) and Eq.(4), machining time (t_2) can be computed starting from the volume (V) to be removed and the material removal rate MRR.

$$t_2 = \frac{V}{MRR} = \frac{V}{d_r \cdot p \cdot f_z \cdot Z \cdot \Omega \cdot 60} \tag{2}$$

Where d_r is the radial depth of cut (tool-workpiece radial engagement, Fig. 3), p is the axial depth of cut, f_z is the feed per tooth and Z is the number of tool teeth (inserts).

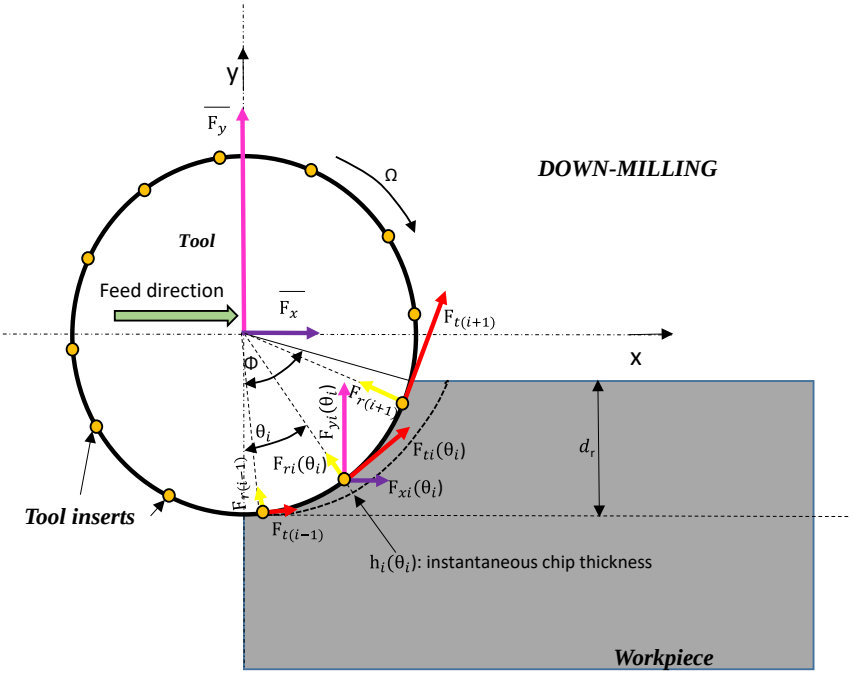

Fig. 3: Schematic representation of the cutting forces (down-milling case) acting on tool inserts an the global effect on the tool along x and y

The spindle speed Ω can be easily computed (Eq.(3)) from the cutting speed v_c that is one of the analyzed process parameters. D is the diameter of the considered tool.

$$\Omega = \frac{v_c \cdot 1000}{\pi \cdot D} \tag{3}$$

The processed blank (Fig. 2) material is geometrically described by the following dimensions: l, b and s. Thus, the volume V can be computed as follows:

$$V = L \cdot b \cdot s \tag{4}$$

According to Eq. (5), t_3 considers the rapid axes motions (e.g. $t_{rapid_{tc}}$ and t_{rapid_m}), the tool-workpiece approaching time ($t_{approaching}$) that depends on feed velocity and the overall time to perform the tool change ($t_{tc} + t_{worker}$).

The workpiece approaching phase was conceived in order to avoid the axes move toward the workpiece with the maximum feed velocity (rapid motions). Approaching movements toward the workpiece are expected both after each tool change and before each rapid movements between two consecutive passes, Fig. 2.

It is also assumed that for each tool change, the machine has to perform two rapid movements "$rapid_{tc}$": one towards the tool changer and the other one back to the workpiece, Fig. 2. Moreover, two rapid movements are necessary to get and to release the tool at the beginning and at the end of the task, Eq.(6). More in detail, n_t is the number of the performed tool changes, n_r the number of rapid movements linked to the tool changes and n_{rp} the number of milling passes. For each tool pass, both an approaching phase (which duration is equal to $t_{approaching}$) and a rapid motion (that lasts t_{rapid_m}) have been assumed. A similar quantity is also defined when the machine performs rapid motions required for the tool changes $t_{rapid_{tc}}$.

$$t_3 = (t_{tc} + t_{worker}) \cdot n_t + \left(t_{rapid_{tc}} + t_{approaching}\right) \cdot n_r + \left(t_{rapid_m} + t_{approaching}\right) \cdot n_{rp} \quad (5)$$

$$n_r = 2 \cdot n_t + 2 \quad (6)$$

Tool life affects t_3 through the number of tool changes n_t. The tool duration ($T_{tool\ life}$) is modelled by the basic Taylor's equation (Eq. (7)) that considers the adopted cutting speed (v_c) and the tool-workpiece material combination through the coefficients C and α. Sandvik Italia provided us the Taylor's parameters for the analyzed tools/materials. According to Eq. (8), the total number of tool changes (n_t) depends on the tool life and on the overall machining time t_2:

$$v_c \cdot (T_{tool\ life})^{\alpha} = C \quad (7)$$

Thus, n_t can be computed using the following equation:

$$n_t = t_2 / T_{tool\ life} \quad (8)$$

In order to remove from the workpiece a layer p [mm] thick (axial depth of cut, Fig. 2), n_p milling passes has to be carried out, Eq. (9). Therefore, the approximated number of milling passes (n_{rp}) for processing the whole volume V can be computed through Eq. (10).

$$n_p = \min\{n \in \mathbb{Z} | n > b/d_r\} \quad (9)$$

$$n_{rp} = (n_p - 1) \cdot \frac{s}{p} \quad (10)$$

In the developed model we considered that the new tool is set-up during machining but, at the same time, that the availability of tools is limited. For instance, if the tool change occurs too frequently (it happens when a very high cutting speed is selected) the machine could be forced to wait for a new tool until it will be loaded on the magazine by the operator. In this case, the operator cannot change the tool without stopping the machining process. For this reason, it is assumed (see Eq. (5)) that the overall time to perform the tool change takes into consideration

both the time connected to the automatic tool changer (t_{tc}) and the average time required by the operator to set up the tool magazine ascribable to each single tool (t_{worker}). In fact, it is not realistic to assume an unlimited tool availability: this is why an extra contribution is summed up to t_{tc}.

As anticipated, $t_{rapid_{tc}}$ is the time spent to move the machine head (at the maximum axis velocity) from the workpiece to the tool change reference point. In this phase the generic j machine axis covers the SRR_j distance. The movement is performed at the maximum velocity (rapid): a trapezoidal speed profile was assumed in order to consider the acceleration and the deceleration phases. $t_{approaching}$ is the time required by the machine to approach and to leave the workpiece before and after each tool change. We assumed that this quantity can be considered at the end of each milling pass and before the following one. In this case, the AD distance (Fig. 2 and Eq. (15)) is covered by the axis at the feed velocity (not rapid).

It is assumed that all the rapid axes movements are performed adopting a trapezoidal velocity profile, see Fig. 4. In the following picture the speed profiles assumed during both the tool change (by the generic j axis) and during the rapid motions between two consecutive cuts (by the x axis). V_{trj} is the maximum axis j speed velocity.

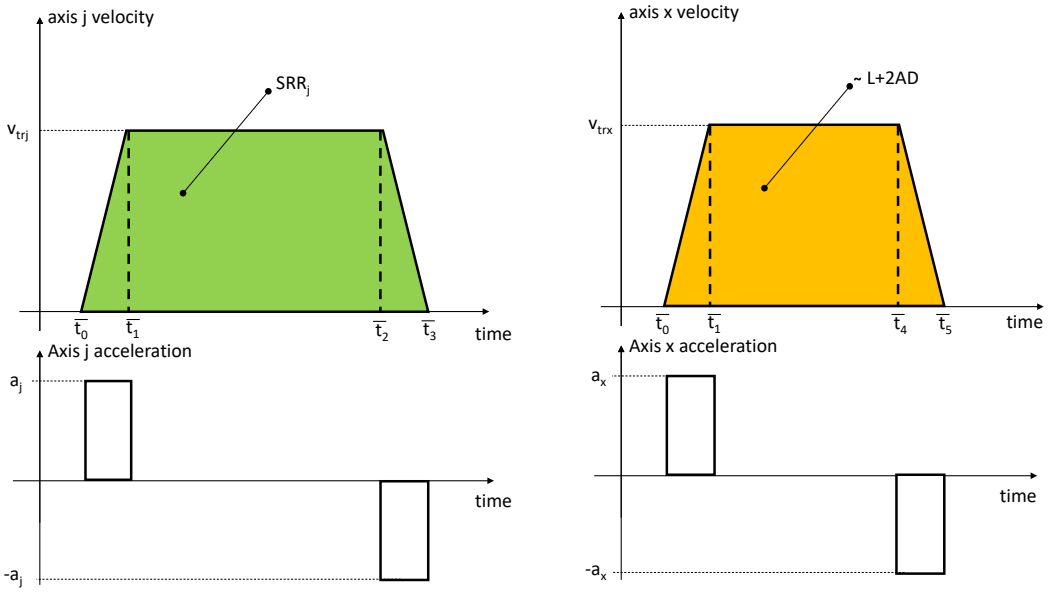

Fig. 4: graphical representation of the rapid axes movements (speed and acceleration profiles)

Both t_{rapid_m} and $t_{rapid_{tc}}$ are computed considering the mentioned assumption, Eq.(11)-(12).

$$t_{rapid_m} = (\bar{t_1} - \bar{t_0}) + (\bar{t_4} - \bar{t_1}) + (\bar{t_5} - \bar{t_4}) \tag{11}$$

$$t_{rapid_{tc}} = (\bar{t_1} - \bar{t_0}) + (\bar{t_2} - \bar{t_1}) + (\bar{t_3} - \bar{t_2}) \tag{12}$$

The distance covered by the generic j axis during rapid motion depends on the specific axis task. For instance, the distance covered by the axis j to perform the tool change can be computed through Eq. (13):

$$\int_{\bar{t_0}}^{\bar{t_1}} a_j \cdot t \cdot dt + \int_{\bar{t_1}}^{\bar{t_2}} v_{tr_j} \cdot dt + \int_{\bar{t_2}}^{\bar{t_3}} \left(v_{tr_j} - a_j \cdot t\right) \cdot dt = SRR_j \tag{13}$$

While Eq.(14) gives the distance covered by the axis in rapid motion between two consecutive milling active passes, refer to Fig. 2. In this specific case a feed motion along the x axis is assumed.

$$\int_{\bar{t_0}}^{\bar{t_1}} a_x \cdot t \cdot dt + \int_{\bar{t_1}}^{\bar{t_4}} v_{tr_x} \cdot dt + \int_{\bar{t_4}}^{\bar{t_5}} \left(v_{tr_x} - a_x \cdot t\right) \cdot dt \cong (L + 2 \cdot AD) \tag{14}$$

Where AD is the distance covered by the tool before and after the active phase, Fig. 2:

$$AD = \frac{D}{2} + e_s \tag{15}$$

And e_s is the extra stroke that allows to properly engage and release the workpiece.

2.2. Energy model development

In this research, the overall energy consumption (E_{total}) in a machine tool is decomposed into three terms, see Eq. (16)-(18). $E_{functional\ modules}$ is the energy consumed by the main machine functional modules (e.g. pallet clamping $E_{pallet\ clamp}$, axes E_{axes}, axes chiller $E_{axes\ chiller}$, spindle chiller $E_{spindle\ chiller}$, chip conveyor $E_{chip\ conveyor}$, tool change system $E_{tool\ changer\ system}$, cutting fluid system $E_{coolantHP}$), $E_{cutting}$ is the energy consumed for processing the material and $E_{stand-by\ power}$ is the energy consumed during the machine stand-by. Stand-by power (P_0) is computed as the sum of the base powers of the modelled machine tool components. It is important to observe that the power contributions of the auxiliaries not directly explicated in the following equations are considered in P_0. It seems reasonable since they are switched on for the whole production duration t. For instance, the average power consumption of the chiller of the electrical cabinet is included in P_0.

$$E_{total} = E_{functional\ modules} + E_{stand-by\ power} + E_{cutting} \tag{16}$$

$$E_{functional\ modules} = E_{axes} + E_{axes\ chiller} + E_{auxiliaries} + E_{tool\ changer\ system} \tag{17}$$

$$E_{auxiliaries} = E_{spindle\ chiller} + E_{chip\ conveyor} + E_{pallet\ clamp} + E_{coolantHP} \tag{18}$$

$E_{stand\text{-}by\ power}$ is due to stand-by power consumption and it is estimated by the multiplication of stand-by power and the total processing time.

$$E_{stand-by\ power} = P_0 \cdot t \tag{19}$$

Focusing on the auxiliaries ($E_{auxiliaries}$), the energy required for the chip conveyor ($E_{chip\ conveyor}$), the pallet clamping system ($E_{pallet\ clamp}$), the spindle chiller ($E_{spindle\ chiller}$) and the cutting coolant system ($E_{coolantHP}$) can be computed using the energy definition and the corresponding power values, Eq.(20).

$$E_{auxiliaries} = (P_{spindle\ chiller} \cdot t_2 + P_{chip\ conveyor} \cdot t_2 + P_{coolantHP} \cdot t_2 + P_{pallet\ clamp} \cdot t) \tag{20}$$

$E_{tool\ changer\ system}$ is calculated through Eq. (21). P_{tc} is the average power absorbed by the tool change system. t_{tc} is the time required to change the tool. n_t is the number of the performed tool changes. During the tool change time, machine does not work but the stand-by power is absorbed in any case, Eq. (19)

$$E_{tool\ changer\ system} = P_{tc} \cdot t_{tc} \cdot n_t \tag{21}$$

E_{axes} is energy consumed due to axes movements, $E_{axes\ chiller}$ is the energy used by the chiller to cool the linear axis motors while $E_{spindle\ chiller}$ is the energy required to cool the spindle. Each machine tool function module is considered active only when it is involved in a specified production task.

In the following subsections more details on each developed specific energy model will be provided.

2.2.1. Constant power machine tool components

As already anticipated, for some functional modules (e.g. chip conveyor, pallet clamp, spindle chiller, tool change system and stand-by power) it was assumed a constant power consumption model. This was confirmed by the experimental power measurements performed on the real machine. The experimental power data were used to get $E_{chip\ conveyor}$, $E_{pallet\ clamp}$, $E_{spindle\ chiller}$, $E_{tool\ change\ system}$, and $E_{stand\text{-}by\ power}$. Even if the absorbed power is constant, the consumed energy depends on the process parameters since they affect the processing time. For instance, $E_{stand\text{-}by\ power}$ and $E_{pallet\ clamp}$ depend upon the whole processing time (t). Specifically, $E_{chip\ conveyor}$ depends on the machining time (t_2) and $E_{tool\ change\ system}$ depends both on the number of tool changes and the time required to perform the tool change.

2.2.2. Cutting Energy

$E_{cutting}$ is the energy required to remove the material. It can be computed exploiting the well-known semi-empirical cutting force model that is based on the cutting pressure K_t (Eq.(22)-(24)), Altintas (2012).

The cutting power can be computed using the following relationship:

$$P_{cutting} = \bar{F_t} \cdot \frac{D}{2} \cdot \Omega \cdot 2\pi/60 = \bar{F_t} \cdot v_c \cdot 1000/60 \tag{22}$$

Thus, the energy required to process the amount of material V is:

$$E_{cutting} = \frac{P_{cutting} \cdot t_2}{\eta} \tag{23}$$

Eq. (23) takes into consideration also the spindle efficiency η that, for sake of simplicity, is assumed constant and not affected by the working conditions.

$\bar{F_t}$ represents the global effect of the tangential forces linked to each engaged tool insert, Fig. 3.

The average global tangential cutting force ($\bar{F_t}$) both for up/down-milling can be computed using the following approximation that exploits the average chip thickness:

$$\bar{F_t} = \sum_{i=1}^{n_{teeth\ effective}} F_{ti}(\theta_i) \cong K_t \cdot h_m \cdot p \cdot n_{teeth\ effective} \tag{24}$$

The cutting pressure K_t can be computed considering the effects of the chip thickness on the specific cutting pressure K_{ts} through the following well-known exponential (w) relationship, Altintas (2012):

$$K_t = K_{ts} \cdot (h_m)^{-w} \tag{25}$$

h_m can be calculated using the following equation, Altintas (2012): . χ is the lead angle

$$h_m = \frac{2 \cdot d_r \cdot f_z \cdot \sin(\chi)}{\Phi \cdot D} \tag{26}$$

In Eq. (24), $n_{teeth\ effective}$ is the average number of engaged tool teeth that can be computed through the following relationship:

$$n_{teeth\ effective} = (\Phi \cdot Z)/(2\pi) \tag{27}$$

The tool engagement angle (Φ) was computed using Eq. (28) and Eq. (29): refer to Fig. 3 for further details.

When $a_e > D_f/2$

$$\Phi = \frac{\pi}{2} + \sin^{-1}((d_r - D/2)/(D/2)) \tag{28}$$

And when $a_e < D_f/2$

$$\Phi = \frac{\pi}{2} - \sin^{-1}((d_r - D/2)/(D/2)) \tag{29}$$

2.2.3. Axis energy model

The energy required for the axes movements (E_{axes}) considers the energy required for all the rapid movements (E_{rapid}), the energy required to approach the workpiece ($E_{approaching}$) and the energy required by the axes during the material removal ($E_{axis\ working}$), Eq. (30).

$$E_{axes} = E_{rapid} + E_{approaching} + E_{axis\ working} \tag{30}$$

Eq. (31) can be used to collect all the contributions of all the axis.

$$E_{axes} = \sum_j E_{axis_j} \tag{31}$$

Before detailing each single term of the above equation, it is necessary to present the power model $P_j(t)$ adopted for the generic j machine axis (x, y and z-directions). The time intervals linked to each energy axis contributions were already defined in section 2.1.

The model considers two terms: mechanical power ($P_{m_j}(t)$) and copper losses ($P_{r_j}(t)$).

$$P_j(\mathrm{t}) = \mathrm{P}_{\mathrm{m}_j}(\mathrm{t}) + \mathrm{P}_{\mathrm{r}_j}(\mathrm{t}) \tag{32}$$

The mechanical power can be computed using the following equation where $\mathrm{v}_{\mathrm{t}_j}(t)$ is the j axis velocity

$$\mathrm{P}_{\mathrm{m}_j}(\mathrm{t}) = \mathrm{F}_{\mathrm{m}_j}(\mathrm{t}) \cdot \mathrm{v}_{\mathrm{t}_j}(\mathrm{t}) \tag{33}$$

Where $\mathrm{F}_{\mathrm{m}_j}(\mathrm{t})$ is the equivalent force that loads the j axis. The axis load can be computed considering the following relationship:

$$\mathrm{F}_{\mathrm{m}_j}(\mathrm{t}) = \left(\mathrm{c}_{\mathrm{s}_j} \cdot \mathrm{sgn}\left(\mathrm{v}_{t_j}(\mathrm{t})\right) + \mathrm{c}_{\mathrm{d}_j} \cdot \mathrm{v}_{t_j}(\mathrm{t}) + \mathrm{M}_{\mathrm{j}} \cdot \mathrm{a}_j(\mathrm{t}) + \mathrm{F}_{\mathrm{j}}(\mathrm{t})\right) = \mathrm{CM}_{\mathrm{j}} \cdot \mathrm{i}_{q_{\mathrm{rms}_j}} \tag{34}$$

The considered axis load contributions are connected to static friction ($\mathrm{c}_{\mathrm{s}_j}$), viscous friction ($\mathrm{c}_{\mathrm{d}_j}$), axis inertia ($\mathrm{M}_{\mathrm{j}}$) and the cutting force ($\mathrm{F}_{\mathrm{j}}(t)$) that acts along the j axis. The axis parameters were identified exploiting experimental tests. The procedure is described in section 3. Depending on the specific axis task, one or more contributions can be neglected. For instance, during the rapid axis motions, the cutting force is generally not applied to the tool and conversely during feed motions, the axis has null acceleration. The force $\mathrm{F}_{\mathrm{m}_j}$ can be also obtained considering the rms (root mean squared) quadrature current absorbed by the motor ($\mathrm{i}_{q_{rms}}$) and the constant of the electrical motor (CM_{j}).

Copper losses ($\mathrm{P}_{\mathrm{r}_j}$) can be computed knowing the electrical resistance of the motor (R_{j}) and the quadrature current ($\mathrm{i}_{\mathrm{q}_j}(\mathrm{t})$) through Joule's law.

$$\mathrm{P}_{\mathrm{r}_j}(\mathrm{t}) = \mathrm{R}_{\mathrm{j}} \cdot (\mathrm{i}_{\mathrm{q}_j}(\mathrm{t}))^2 \tag{35}$$

Where:

$$\mathrm{i}_{q_{\mathrm{rms}_j}} = \mathrm{i}_{\mathrm{q}_j}(\mathrm{t})/\sqrt{2} \tag{36}$$

The axis velocity ($\mathrm{v}_{\mathrm{t}_j}(\mathrm{t})$) depends on the specific considered axis task

For instance, during the axis feed motion the velocity can be computed using the following relationship. The axis velocity was assumed constant for each single pass.

$$\mathrm{v}_{\mathrm{t}_j} = \mathrm{f}_{\mathrm{z}_j} \cdot \mathrm{z} \cdot \Omega \cdot \frac{60}{1000} \tag{37}$$

On the other hand, when the axis performs rapid movements ($\mathrm{E}_{\mathrm{rapid}}$), three phases need to be considered. As reported in Fig. 4, a trapezoidal axis speed profile was assumed. In the first phase the axis accelerates up to the constant rapid speed (time interval $(\bar{t_1} - \bar{t_0})$), in the intermediate phase the axis moves at constant rapid speed $\mathrm{v}_{\mathrm{tr}_j}$ (time interval $(\bar{t_2} - \bar{t_1})$ or $(\bar{t_4} - \bar{t_1})$ depending on the length of the axis stroke) and in the last phase the axis decelerates up to stand still (i.e. time interval $(\bar{t_3} - \bar{t_2})$ or equivalently $(\bar{t_5} - \bar{t_4})$). In the $\mathrm{E}_{\mathrm{rapid}_{\mathrm{j}}}$ computation, not only the axes rapid motions necessary to change the tools are considered but also the rapid motions necessary to implement the described machining strategy (Fig. 2) were taken into consideration through n_{rp}.

2.2.3.1. Energy axis model for rapid motions

Thus, referring to a generic axis j, the E_{rapid_j} can be calculated with Eq. (38).

$$\begin{aligned} E_{rapid_j} = n_r \cdot \Bigg(& \int_{t_0}^{t_1} P_{acc_j}(t) \cdot dt + \int_{t_1}^{t_2} P_{rapid_j}(t) \cdot dt + \int_{t_2}^{t_3} P_{dec_j}(t) \cdot dt + \int_{t_0}^{t_1} P_{r_j}(t) \cdot dt \\ & + \int_{t_1}^{t_2} P_{r_j}(t) \cdot dt + \int_{t_2}^{t_3} P_{r_j}(t) \cdot dt \Bigg) + n_{rp} \\ & \cdot \Bigg(\int_{t_0}^{t_1} P_{acc_j}(t) \cdot dt + \int_{t_1}^{t_4} P_{rapid_j}(t) \cdot dt + \int_{t_4}^{t_5} P_{dec_j}(t) \cdot dt \\ & + \int_{t_0}^{t_1} P_{r_j}(t) \cdot dt + \int_{t_1}^{t_4} P_{r_j}(t) \cdot dt + \int_{t_4}^{t_5} P_{r_j}(t) \cdot dt \Bigg) \end{aligned} \tag{38}$$

Where $P_{acc_j}(t)$, $P_{rapid_j}(t)$ and $P_{dec_j}(t)$ are respectively the mechanical power absorbed by the j axis during the acceleration phase, during the movement at the maximum feed velocity and during the deceleration phase.

E_{rapid_j} can be computed considering the equivalent load of each axis $F_{m_j}(t)$ (not taking into account the contribution due to the cutting forces) and Eq. (39)- Eq. (40) that express the axis velocity during the acceleration (a_j) and the deceleration ($-a_j$) phases.

$$v_{t_j}(t) = a_j \cdot t \tag{39}$$

$$v_{t_j}(t) = v_{tr_j} - a_j \cdot t \tag{40}$$

In the axes deceleration phase (motor breakage) we have assumed to recover only a portion (β) of the kinetic energy of the axis.

2.2.3.2. Energy axis model for approaching motions

Regarding the approaching movements, both the phases in which the tool enters and exits the workpiece at feed velocity were taken into consideration. Since it was assumed that during these phases the axes move at feed velocity v_{t_j}(Eq. (42)) therefore $E_{approaching}$ can be computed using a simplified release of Eq. (34). In this case only the energy linked to the axis motion (time interval $t_{approaching}$) at feed velocity has been considered, Eq.(41). In such a time interval, the distance covered by the axis at v_{t_j} is equal to AD, Eq. (42).

$$\begin{aligned} E_{approaching_j} = & \left(n_r + 2 \cdot n_{rp}\right) \\ & \cdot \Bigg(\int_0^{t_{approaching}} \left(c_{s_j} \cdot \mathrm{sgn}\left(v_{t_j}\right) + c_{d_j} \cdot v_{t_j}\right) \cdot v_{t_j} \cdot dt \\ & + \int_0^{t_{approaching}} P_{r_j}(t) \cdot dt \Bigg) \end{aligned} \tag{41}$$

$$AD = \int_0^{t_{approaching}} v_{t_j} \cdot dt \tag{42}$$

2.2.3.3. Energy axis model for machining phases

When the machine is removing material from the workpiece, the cutting forces load the axes therefore the $F_j(t)$ term in Eq. (34) has to be considered. In this paper, an analytical approach to compute the cutting forces along x-axis and y-axis directions was formulated for up/down milling cases. This allows analyzing the effects of different cutting parameters/strategies selection on the power consumption of the machine axes and consequently on the overall absorbed energy. This aspect represents a novelty with respect to other research works.

It was demonstrated (performing numerical simulations with the CutPro Sofware, CutPro Guide) that the adopted average approach in the tangential cutting force computation $\overline{F_t}$ (Eq. (24)-(26)) brings to a very accurate estimation of the average cutting torque and power. For brevity, we did not reported the simulated results. Maximum observed error in the average tangential force computation is less than 10% (when the radial depth of cut is minimum).

The average approach was also extended to compute the overall average forces along x and y ($\overline{F_x}$ and $\overline{F_y}$).

Considering the mechanistic model (Altintas, 2012), the tangential $F_{ti}(\theta)$ and radial $F_{ri}(\theta)$ cutting forces acting on each single engaged tooth (Fig. 3) can be computed with the following equations:

$$F_{ti}(\theta) = K_t\big(h_i(\theta_i)\big) \cdot p \cdot h_i(\theta_i) \cong K_t(f_z) \cdot p \cdot f_z \cdot \sin\theta_i \tag{43}$$

$$F_{ri}(\theta) = K_r\big(h_i(\theta_i)\big) \cdot p \cdot h_i(\theta_i) \cong K_r(f_z) \cdot p \cdot f_z \cdot \sin\theta_i \tag{44}$$

For sake of simplicity, the dependence of K_t (tangential cutting pressure) and K_r (radial cutting pressure) on the instantaneous chip (see Eq.(25)) was neglected. This brings to a small approximation. The maximum difference in the average force computation is less than 10%. It was numerically verified.

Thus, $\overline{F_x}$ (in this specific case it is the feed force) and $\overline{F_y}$ can be computed both for up-milling and down-milling operations

For up milling

$$\begin{aligned}\overline{F_x}_{\text{up milling}} &= n_{\text{teeth effective}} \cdot \left(\frac{1}{\Phi}\int_0^{\Phi} (-F_{ti}(\theta_i)\cos\theta_i - F_{ri}(\theta_i)\sin\theta_i) \cdot d\theta_i\right) = \\ &= n_{\text{teeth effective}} \left(\frac{K_t(f_z) \cdot f_z \cdot p}{\Phi} \cdot \left(-\frac{1}{4} + \frac{1}{4}\cos 2\Phi\right) - \frac{K_r(f_z) \cdot f_z \cdot p}{\Phi} \right. \\ &\left. \cdot \left(\frac{1}{2}\Phi - \frac{1}{4}\sin 2\Phi\right)\right)\end{aligned} \tag{45}$$

$$\overline{F_{y}}_{\text{up milling}} = n_{\text{teeth effective}} \cdot \left(\frac{1}{\Phi} \int_{0}^{\Phi} (-F_{ti}(\theta_i)\sin\theta_i + F_{ri}(\theta_i)\cos\theta_i) \cdot d\theta_i \right)$$
$$= n_{\text{teeth effective}} \left(\frac{K_t(f_z) \cdot f_z \cdot p}{\Phi} \cdot \left(-\frac{1}{4} + \frac{1}{4}\cos 2\Phi \right) - \frac{K_r(f_z) \cdot f_z \cdot p}{\Phi} \cdot \left(\frac{1}{2}\Phi - \frac{1}{4}\sin 2\Phi \right) \right) \quad (46)$$

Eq. (45)-(46) show the dependence of the average forces acting on machine tool axes on the main cutting parameters: radial depth of cut d_r, axial depth of cut p and feed f_z. Similar equations can be developed also for down-milling operations.

As an example, the effects of radial depth of cut on both $\overline{F_x}$ and $\overline{F_y}$ are shown in Fig. 5.

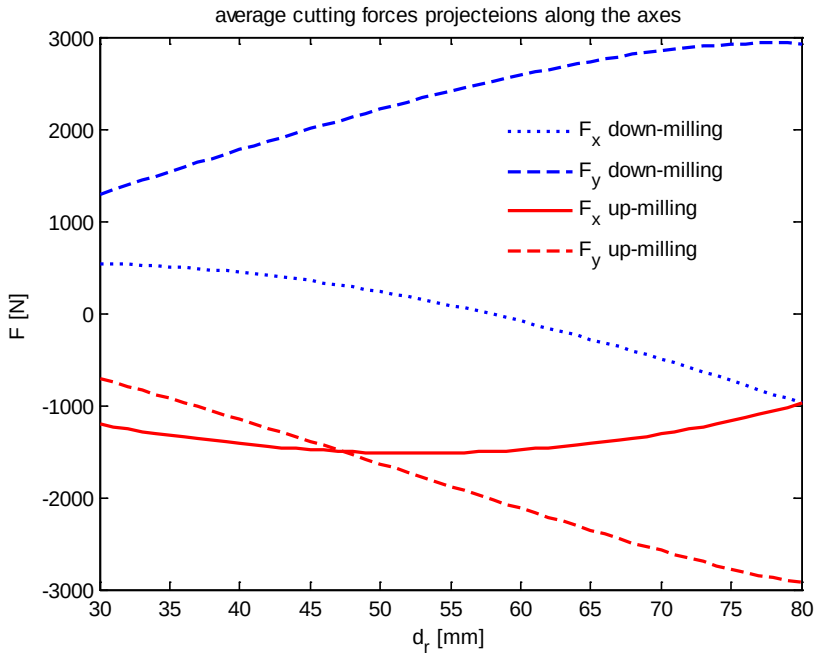

Fig. 5: Effects of ae example on the average cutting forces projections $\overline{F_x}$ and $\overline{F_y}$ (up/down milling)

Finally, the energy absorbed by the machine axes during the material removal can be expressed as follows where $\overline{F_j}$ is the average force along the generic machine axis j.

$$E_{\text{axis working}_j} = \left(\left(c_{s_j} \cdot \text{sgn}\left(v_{t_j}\right) + c_{d_j} \cdot v_{t_j} + \overline{F_j} \right) \cdot v_{t_j} + \left(\frac{\left(c_{s_j} \cdot \text{sgn}\left(v_{t_j}\right) + c_{d_j} \cdot v_{t_j} + \overline{F_j} \right)}{K_{tj}} \right)^2 \cdot 2R_j \right) \cdot t_2 \quad (47)$$

Considering the analyzed cutting strategy Fig. 2, the axis velocity is not null ($v_{t_j} \neq 0$) only for the feed direction.

2.2.4. Chiller axes energy modelling

Regarding the chiller of the machine axes, ($E_{axes\ chiller}$), a simple model was chosen for this component. We assumed that the axis chiller exhibits a power consumption that linearly depends on the power losses of the axes motors. A basic power (P_{sbv}) was also considered. The linear term depends on the overall Joule losses through δ, Eq. (48).

$$E_{axes\ chiller}(t) = P_{sbv} \cdot t + \delta \cdot \left(\sum_j \sum_q \left(P_{r_{jq}} \cdot t_q \right) \right) \quad (48)$$

The higher is the axes power consumption (copper losses) the higher is the power consumption of the chiller because it increases its duty cycle. In Eq.(48), ($P_{r_{jq}}$) is the dissipated power due to copper losses by each single axis j during a generic task (i.e. rapid, feed, machining) that lasts t_q seconds. For sake of simplicity, we took into account the $E_{axes\ chiller}$ when the axes move at constant speed (both at feed and rapid velocity) and not during acceleration/deceleration phases.

3. Experimental tests and model parameters identification

In order to tackle the energy minimization, some of the parameters of the developed model need to be defined (e.g. tool properties, workpiece properties (geometry and material), etc). Moreover, reasonable technological ranges for the variable (a_e, a_z and v_c) analyzed in the constraint optimization were also defined, Table 1. This allows to define the technological scenario in which perform the energy minimization. Since the axial depth of cut p generally depends on the machine tool dynamic performance (due to vibration issues) it is kept constant at its maximum value. Moreover, a high alloy steel was the first material considered in the analysis.

Table 1: Cutting parameter ranges, workpiece dimensions, workpiece material properties and tool specifications

Cutting parameters range	**Values (units)**	**Workpiece dimensions (rectangular block)**	**Values (units)**
Radial depth of cut (d_r)	30-80 [mm]	Workpiece length (l)	400 [mm]
Feed rate per tooth (f_z)	0.1-0.3 [mm]	workpiece width (b)	500 [mm]
Cutting speed range (v_c)	140 to 350 [m/min]	Thickness of the volume to be removed (s)	12 [mm]
Axial depth of cut (p)	4 [mm]	AD	45 [mm]
Workpiece material properties	**Values (units)**	SRRx, SRRy , SRRz	700, 700, 800 [mm]
Workpiece material	High alloy steel	**Tool parameters**	**Values (units)**
Specific cutting pressure (K_{ts})	1950 [N/mm^2]	Lead angle (χ)	90 [degree]
Specific cutting pressure coefficient (w)	0.152	Taylor coefficient (α)	0.25
-	-	Taylor constant (C)	360 [m/min]
-	-	Tool diameter (D)	80 [mm]
-	-	Number of tool inserts (Z)	6

Some other parameters of the model were identified exploiting experimental tests. The experimental measurements were performed on a CNC machine tool equipped with linear axes and an electro spindle. The

analyzed machine is suitable for processing various materials even if it is more adequate for aluminum and steel alloys. The tested machine was specifically design for mass production since it was equipped with linear motors, automatic tool and workpiece changers.

In order to identify the main machine parameters used in the developed model, different tests were carried out:

- Experimental measurements through the machine Numerical Controller (e.g. for the axis parameters identification). The adopted identification procedure was described more in detail in Albertelli et al. (2011).
- Energy measurements for the direct identification of some parameters of the energy model (e.g. stand-by power, tool changer power, etc.)
- Energy measurements performed according to a defined procedure in order to identify the parameters of the chiller model

Other model parameters were found performing further tests (for instance measuring the automatic tool change duration or the motor electrical resistance) or looking at the machine components specification catalogues. For instance, some data concerning the electrical motors were found in the connected technical documentation.

For instance, in the axis model, three main parameters were identified: axis inertia (M_j), static friction coefficient (c_{s_j}) and viscous friction coefficient (c_{d_j}). The motor quadrature current and the axis kinematics were acquired during a specifically designed axis cycle that includes linear interpolation motion (both with rapid (G00 – G code) and feed velocity (G01 – G code)) and circular interpolations (G02). The axis cycle used for the characterization did not include machining phases, thus $F_j(t) = 0$. The measured quadrature current i_q (experimentally acquired through the machine Siemens drive) was fitted with a regression (Least Square Regression) equation to get the desired parameters. Since during the characterization campaign the axis kinematics was also acquired by the drives and the motor resistance was experimentally measured, the unique unknown parameters of Eq. (34) are c_{s_j}, c_{d_j}, M_j that can be easily determined through the regression procedure.

Fig. 6 shows the comparison between the measured quadrature current (x - axis motor) and the estimation performed with the updated axis model. The estimated current (proportional to the force) was computed using the measured axis kinematics (got from the Siemens drive) and the identified parameters, Eq.(34). Fig. 6 shows that the adopted model allows reproducing quite accurately the experimental results (motor quadrature current).

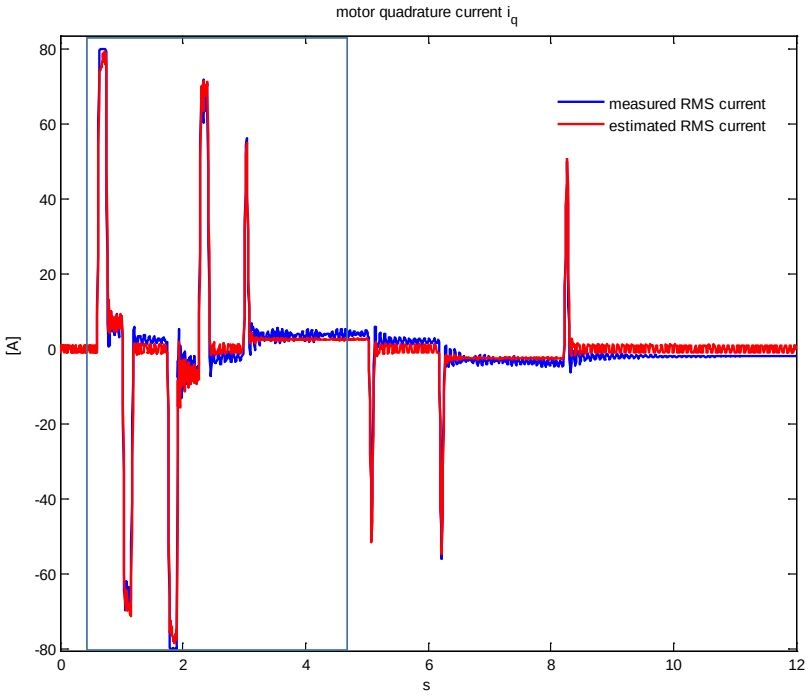

Fig. 6: Experimental-Numerical comparison – quadrature current absorbed by the x-axis

To verify the axes energy consumption model, the power computed by the model (Eq. (34)) was compared with the power measured through the power meter installed on the axis drive, as in Fig. 7.

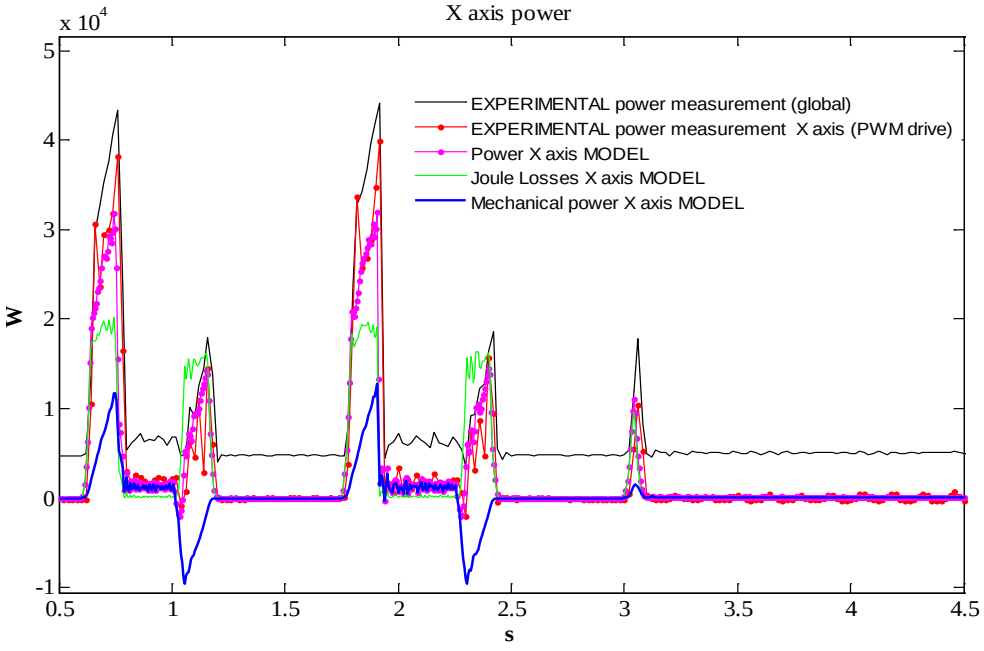

Fig. 7: Power absorbed by the x-axis during the characterization procedure, experimental-analytical comparison. The main power contributions considered in the model are also reported.

The comparison is shown only for a portion of the overall tested cycle; refer to the rectangle reported in Fig. 6. Two subsequent rapid axis motions and a portion of the feed motion were analysed. Focusing on the first axis rapid motion (e.g. from 0.6 second to 1.2 second (Fig. 7)), x-axis starts accelerating from a stand still condition up to a constant rapid speed, then it moves with a constant rapid speed for a while and then it decelerates up to zero velocity. The highest power consumption peak was observed in the acceleration phase. During the deceleration phase (axis breakage), the absorbed power is lower because the contribution linked to the mechanical energy is recovered (negative power). It can be noted that the overall power continues being positive due to the role of the Joule losses, Fig. 7. The results reported in Fig. 7 confirm that the model can quite accurately predict the axes power consumption. The energy consumption linked to an axis rapid movement was computed and compared with the one coming from experimental data: the error is limited to 8% thus the result seems acceptable for the paper purposes. The model parameters identification approach was also adopted for the other machine tool axes.

The described axes-chiller model is based on a linear dependency between the global axes joule losses and the power absorbed by the chiller, Eq. (48). Higher the axis motor Joule losses, higher the energy spent by the chiller to cool the motor. Indeed, in order to identify the axis chiller basic power (P_{sby}) and the coefficient of the linear term δ, some experiments were carried out. The experiments were performed changing the chiller loading conditions: three loading conditions were reproduced. Specifically, the axis duty cycle was increased in order to increase the copper losses and consequently the chiller consumption. During the characterization tests the electrical power of both the chiller and the axes were acquired. For all the tested conditions, the Joule losses linked to the axes motors and the corresponding chiller average powers were computed and reported in Fig. 8.The least square regression technique was used to fit the experimental data with the proposed linear model. Since the coefficient of multiple determination is equal to R^2=0.998, the proposed linear model seems appropriate. Since such a tests are time consuming (for each loading condition the thermal equilibrium needs to be found), an additional verification on the energy consumed by the chiller considering a further loading condition was not carried out.

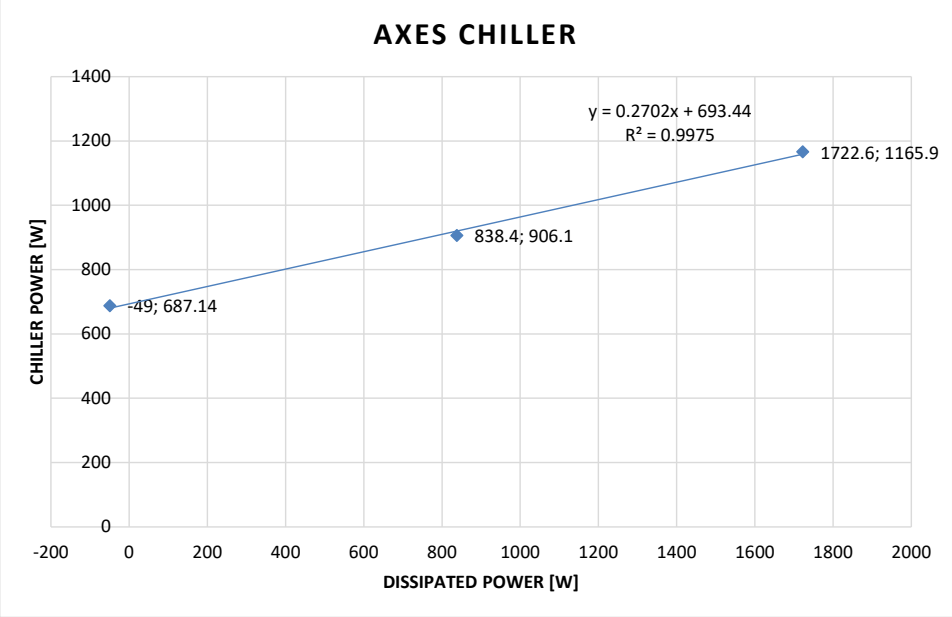

Fig. 8: Axes chiller experimental characterization – model parameters identification

Some parameters of the overall energy model were identified using dedicated power measurements (for instance the energy absorbed by the tool changer system or the stand-by power). In Table 2, the main parameters used in the proposed energy model are summarized.

Table 2: Identified machine parameters

Machine parameters (adopted nomenclature)	**Values (units)**	**Machine parameters** (adopted nomenclature)	**Values (units)**
Static coefficients of the axes x, y and z ($c_{s_x}, c_{s_y}, c_{s_z}$)	128, 87.3, 70.8 [N]	Machine tool stand-by power (P_0)	4865 [W]
Dynamic coefficients of the axes x, y and z ($c_{d_x}, c_{d_y}, c_{d_z}$)	572.7,433.7, 712.4 [N.s/m]	Power absorbed by the tool change system (P_{tc})	80 [W]
Equivalent mass of the axes x, y and z (M_x, M_y, M_z)	1008.3, 286.4, 685.9 [Kg]	Power absorbed by the clamping pallet(P_{clamp})	556.8 [W]
Acceleration of the axes x, y and z (a_x, a_y, a_z)	7.66, 7.66, 7.66 [m/s^2]	Power absorbed by the chip conveyor($P_{chip-conveyor}$)	250 [W]
Linear axes motor constants, axes x, y and z CM_x, CM_y, CM_z)	128.09, 94.3, 111.19 [N/A_{rms}]	Spindle motor efficiency (η)	0.95
Linear axes motor resistance, axes x, y and z (R_x, R_y, R_z)	1.6, 1.6, 1.6 [Ohm]	Automatic tool change duration (t_{tc})	8 [s]
Stand-by power of the axis chiller ($P_{axes-chiller}$)	693.44 [W]	Average Time taken by the worker for setting the tool magazine (t_{worker})	120 [s]
Setup time (t_1)	15 [s]	Axis Chiller: basic power (P_{sby})	693.44 [W]
Axis chiller: linear coefficient (δ)	0.2702	Energy recovery efficiency (β)	0.9
		Cutting fluid system [W] at 20bar	1025W

4. Energy consumption optimization results

Before performing the multivariable energy optimization, additional model settings were presented in this paper section. Moreover, some preliminary analysis considering only the effects of the cutting velocity on the consumed energy were outlined.

4.1. Energy optimization through cutting speed selection

The developed energy consumption model in section 2 was utilized to estimate the total energy consumption (E_{total}) and all the linked energy contributions ($E_{tool\ change\ system}$, E_{axes}, $E_{axes\ chiller}$, $E_{stand\text{-}by\ power}$, $E_{cutting}$, and $E_{auxiliaries}$). In order to assure the absolute independence of the performed analysis to the workpiece dimension, the specific energy SE_{total} is defined as the energy necessary to process a unit volume of material, Eq.(49).

$$SE_{total} = SE_{cutting} + SE_{axes} + SE_{axes\ chiller} + SE_{auxiliaries} + SE_{stand-by\ power} \quad (49)$$

$$= (E_{cutting} + E_{axes} + E_{axes\ chiller} + E_{auxiliaries} + E_{stand-by\ power})/V$$

In Fig. 9, the main contributions of SE_{total} are plotted varying the adopted cutting speed. Other cutting parameters were set as follows: d_r =80 mm, f_z =0.20 mm, p=4mm (up-milling case).

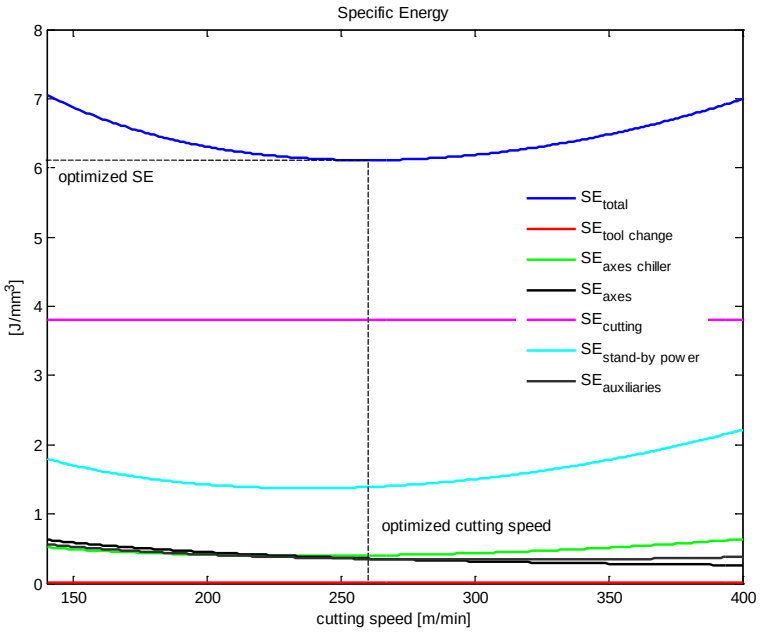

Fig. 9: Specific Energy and its main contributions plotted varying the cutting speed.

Similarly, the Specific Processing Time (SPT or 1/MRR) is the time required to process the unit volume of material. According to Eq.(50), the main contributions are the specific time linked to the piece setup (ST_{t_1}), the specific time linked to the chip-to-chip movements (ST_{t_3}) and the specific time linked to the machining time (ST_{t_2}).

$$SPT = ST_{t_1} + ST_{t_2} + ST_{t_3} = \frac{t_1 + t_2 + t_3}{V} \tag{50}$$

All the considered terms (ST_{t_1}, ST_{t_2} and ST_{t_3}) are plotted in Fig. 10 varying the adopted cutting speed.

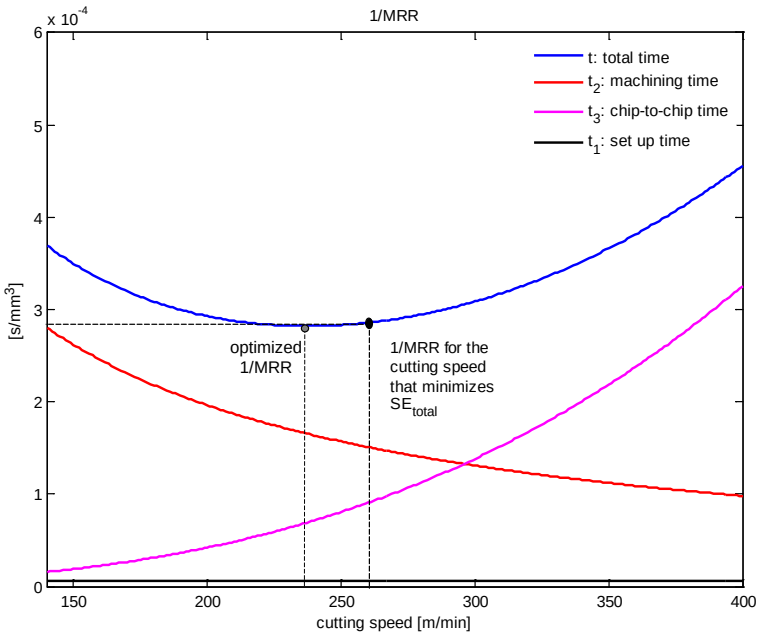

Fig. 10: Specific Processing Time and its main contributions plotted varying the cutting speed.

Since the cutting velocity range is limited, a minimum can be numerically found both for the SE_{total} (OSE Optimized Specific Energy) and for the SPT, Fig. 9 and Fig. 10.

Looking at Fig. 9, it can be observed that SE_{axes}, $SE_{stand\text{-}by\ power}$, $SE_{cutting}$ and $SE_{axes\ chiller}$ are the main energy contributions of the SE_{total}. Other terms can be considered negligible. In addition, the following considerations can be outlined:

- Increasing the cutting speed, $SE_{stand\text{-}by\ power}$ initially decreases and then increases following the SPT trend, Eq. (19) and Eq. (50). Indeed, for low cutting speeds, the SPT is mainly affected by ST_{t_2} (machining time) while for high cutting speeds, ST_{t_3} becomes the more relevant contribution of the SPT.
- $SE_{axes\text{-}chiller}$ exhibits a similar behavior mainly due to the P_{sby} that is absorbed for the whole processing time.
- Specific machining energy ($SE_{cutting}$) is constant due to the combined effect of the cutting velocity on both ST_{t_2} and on the cutting power $P_{cutting}$ (Eq. (2)-(3) and (23)).
- The SE_{axes} decreases with the increment of the cutting speed. This is due to the fact that the both the increment of the energy spent to accomplish a higher number of tool changes (E_{rapid}, Eq. (7), Eq. (8)), Eq. (38) and the increment of the absorbed power (Eq. (47)) are less relevant than the reduction of $E_{axis\ working}$ (Eq. (47)) strictly connected to the machining time t_2 reduction, Eq. (2). This effect would be even more evident in a machine tool with axes powered by traditional rotating electrical motors. In fact, in machine tool equipped with linear motors, the Joule losses (Eq.(35)) have generally a stronger impact on axes energy consumption. This is caused by the absence of any torque amplification (no mechanical transmission) that involves, given a certain axis load (Eq. (33)), a higher current absorption with respect to a rotating servomotor. As already stated, the developed model allows performing these interesting analyses.

Analyzing Fig. 10, it can be seen that the cutting velocity that minimizes the SE_{total} is slightly different from the velocity that minimizes the SPT (260m/min Vs 237m/min). Even the corresponding SE_{total} (6.112J/mm3 Vs

6.138J/mm3) and SPT (2.857E-4 s/mm^3 Vs 2.821E-4s/mm^3) values differ, Fig. 9 and Fig. 10. This is mainly due to the contribution of some of the modelled machine tool functional modules, for instance the machine axes and the axes chiller. Moreover, since the energy absorption of all the axes related machine components depends on the main cutting parameters, a multivariable energy optimization is proposed.

4.2. Multi-variable energy consumption optimization results

In this subsection, the multi- cutting parameter optimization (d_r, p and v_c) was performed exploiting the model described in section 2.2.

Since the model considers a quite realistic machining scenario (e.g. the wear of the tool, the tool changes, the cutting strategy and many contributions to the absorbed energy during both machining and passive phases), it would be interesting to analyze the results of the optimization carried out through a multi-dimensional exhaustive enumeration method.

The OSE (Optimized Specific Energy) was plotted for several process conditions by varying the feed per tooth and the radial depth of cut. The axial depth of cut was kept constant. For each feed/radial depth of cut combination, the plotted SE_{total} is the lowest according to the allowable cutting speeds. For up-milling case, OSE surface plots are shown in Fig. 11(a). The corresponding optimal-cutting speeds are reported in Fig. 11(b): this is the cutting speed that minimizes the global SE for each radial depth of cut-feed combination. In Fig. 11(c) it is reported the percentage of the SE_{total} used for processing the unit of volume ($\eta_{cutting} = SE_{cutting}/SE_{total}$). Such a ratio is an indicator to describe the efficiency of both the machine tool and the machining strategy. High percentage of energy utilization in metal removal is always desirable for highly efficient machine tools. On the other hand, the $(SE_{total} - SE_{cutting})/SE_{total}$ ratio represents the fraction of energy directly connected to non-cutting related machine tool tasks. Many machine tool design choices can therefore affect the above-mentioned ratios. Similarly, in Fig. 11(d) it is reported the percentage of the SE_{total} absorbed by the machine tool axes. It can be observed that the percentage related to SE_{axes} is gradually increasing when the cutting condition becomes heavier (e.g. increasing the MRR). In fact, increasing the cutting parameters, the specific processing time (SPT) gradually decreases, Fig. 11(e) and this has predominant effect on the SE_{total}. Even if this consideration was already reported in some preliminary study that used a simplified machine model (i.e. Rajemi et al. (2010)), in this scenario the result was not easily forecasted due to the model complexity. Indeed, in the developed model, the energy consumption of some machine tool components (e.g. machine axes and related components) increases with the MRR increment (Fig. 11(d)) therefore several trade-offs needed to be evaluated.

In order to better analyse the obtained results, four different process conditions (PC1-upmilling, PC2-upmilling, PC3-upmilling and PC4-upmilling) were highlighted on the surface plot in Fig. 11(a). These four process conditions are utilized to analyze the impact of feed rate and radial depth of cut on the overall specific energy consumption and on the overall specific processing time.

At point PC3-upmilling the OSE is minimum and at point PC2-upmilling the OSE is maximum (Fig. 11 a). When radial depth of cut is increased moving from point PC2-upmilling to PC4-upmilling, OSE reduces by 43%, however, the noticed decrement in the processing time is 62%. Similarly, when radial depth of cut is increased form point PC1-upmilling to PC3-upmilling, OSE reduces by 26% and the processing time reduces by 60% which is less if compared with the reduction observed when feed is set to a lower value. The increment of the radial depth of cut can be the more promising approach for reducing the SE_{total} when feed is set at low values. This guideline could be applied for instance when strict specifications on the surface quality of the processed workpiece are set.

If cutting parameters (feed and/or radial depth of cut) increase, optimum cutting speed increases too (Fig. 11 b). It means that for heavier cutting conditions, the minimum energy consumption is obtained at relatively higher cutting speed. It can be also observed that the increment of both the feed per tooth and the radial depth of cut

simultaneously bring to the increment of the exes energy contribution (up to 9% of SE_{total}, Fig. 11(b)) but, at the same time, to the increment of the overall efficiency (close to 66.2%, Fig. 11(c)).

According to the obtained results, it can be also stated that for all the tested conditions, the SPT is not the minimum achievable one because the energy minimization criteria leads to a different optimized cutting velocity, see also Fig. 10. This is also true for the SPT corresponding to “PC3-upmilling”.

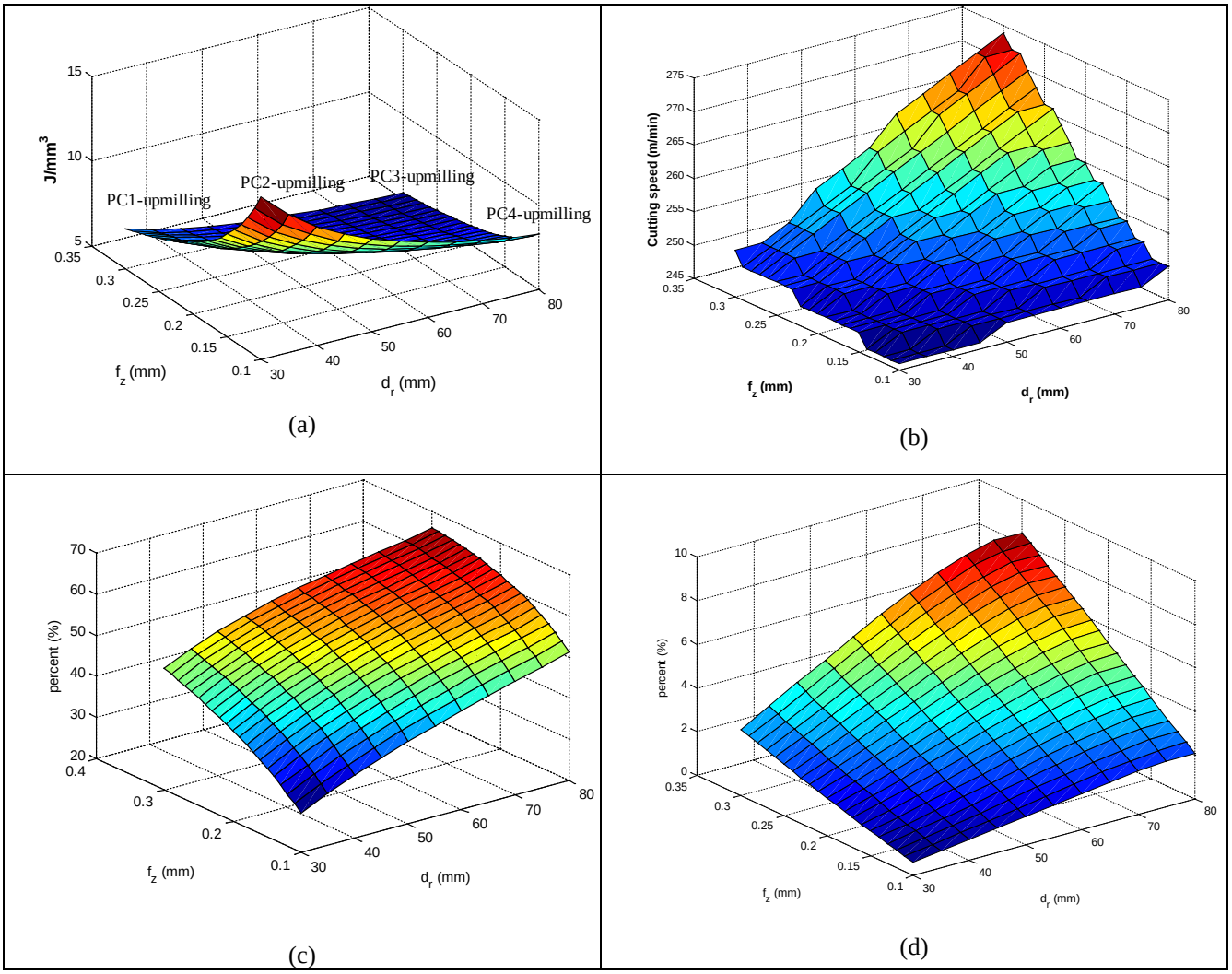

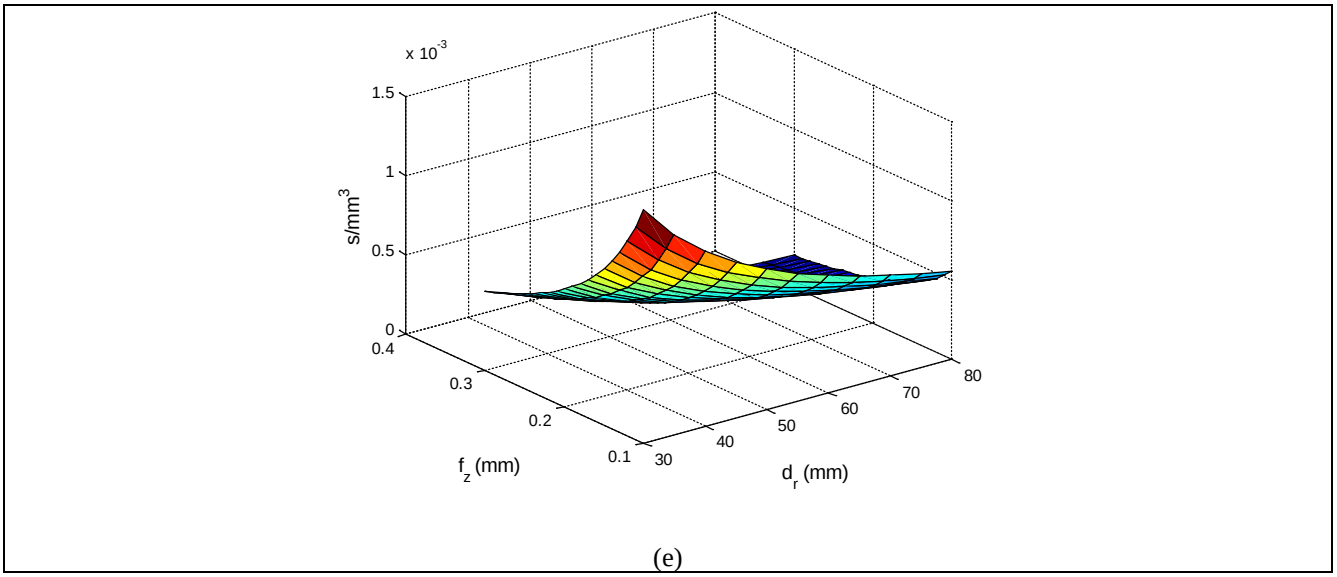

(e)

Fig. 11: The up-milling case study when the process condition is changed by varying feed rate and radial depth of cut: (a) Optimized Specific Energy plot, (b) corresponding optimal cutting speed plot, (c) percentage energy used in removal($\eta_{cutting}$), (d) percentage energy absorbed by axes module ((SE_{axes}/SE_{total})*100), (e) corresponding 1/MRR plot.

In down-milling case, the OSE follows quite similar pattern as such in up-milling case because the differences are mainly connected to energy absorbed by the axis related modules. Even if cutting forces are quite different compared to up-milling (for intermediate d_r), the effect on the SE_{total} is limited.

5. Simulations and results discussion

The developed machine tool energy model was used to perform several simulations in which the $\eta_{cutting}$ ratio, the percentage of specific energy ascribable to the axes, the optimized SE_{total} and the linked SPT were evaluated. The simulations aim at analyzing different feasible and interesting scenarios. For instance, the model was used to emulate both different hypothetical production contexts and various machine tool configurations. For each analyzed scenario, different processed materials (high alloy steel, aluminum and titanium alloys) were considered. Both the parameters associated to the material and to the tool life were opportunely changed for each test case.

Regarding the machine tool configuration, the simulations were performed considering different machine stand-by power values. The nominal value is reported in Table 2. The reduction of machine tool stand-by power consumption is considered, according to recent researches and studies, the easiest and the most effective approach for energy saving in machine tools. Thus, it is quite easy to foresee that the next generation of machine tool will be characterized by a lower basal power consumption.

On the other hand, different production contexts were emulated changing the workpiece set-up time t_1. The nominal value is reported in Table 2. The results reported in the previous paper section refer to a highly automated production in which the workpiece setup is typically performed while another workpiece is being processed and therefore t_1 only takes into account the time spent to automatically change the pallet. Simulations considering higher set-up times were performed. This allows emulating lowly automated production scenarios.

Results of simulations are reported in Fig. 12.

First focusing on the simulations results got decreasing the machine stand-by power. The $\eta_{cutting}$ cutting increment can be appreciated for all the considered working materials even if the highest $\eta_{cutting}$ values can be obtained only when aluminum alloys are machined. Since the achievable MRR (1/SPT) in aluminum milling is considerable higher, the energy contribution of other machine tool functional modules is substantially lower. This can be verified also observing the percentage values connected to the specific energy absorbed by the axes module. For other working materials the axes contribution is significantly higher. The above energy related considerations on axes role are in accordance with the common industrial practice. Indeed, machine tool axes powered by linear motors are particularly suitable for processing light-alloys material. The low $\eta_{cutting}$ values are not only caused by the machine axes but they depend also on the contribution of other machine auxiliaries. High increments in $\eta_{cutting}$ can be observed if the stand-by power is dramatically reduced. Lower $\eta_{cutting}$ enhancements can be achieved reducing the stand-by power when steel and titanium are processed. The reduction of the basal machine tool power will bring to a slight increment in the optimal cutting velocity that minimizes the global consumed energy. As a consequence, the linked SPT increases. Even reducing the stand-by power, the energy minimization can be guaranteed only setting the feed and the radial depth of cut at the maximum allowable values that also entails the production time (SPT) reduction. Even in this analysis, the energy-oriented optimized cutting velocity slightly differs from the velocity that minimizes the production time as already reported in Fig. 10.

Finally, we can also state that many of the well known machine tool design criteria and machining strategies that aim at enhancing the production rate are in accordance with energy reduction oriented policies even if they do not guarantee a proper energy consumption minimization.

In Fig. 12 are also reported the achieved results considering different production scenarios that are simulated setting different workpiece set-up times. The simulations were performed in order to extend the results reported in the previous section. The most evident effect can be observed when the processed material is aluminum. In this case, the setting-up time increment ($10t_1$) brings to a $\eta_{cutting}$ reduction of 18%. This is mainly due to the relevant effect of the set-up time increment on the SPT that was originally very low. For the other processed materials, the t_1 increment involves limited $\eta_{cutting}$ reductions (less than 5%).

The performed simulations are quite useful, they allow emulating various scenarios from the energy consumption perspective extending the validity of the performed considerations. They demonstrated the utility of the developed model.

	Dependence on P_0	Dependence on t_1
$\eta_{cutting}$	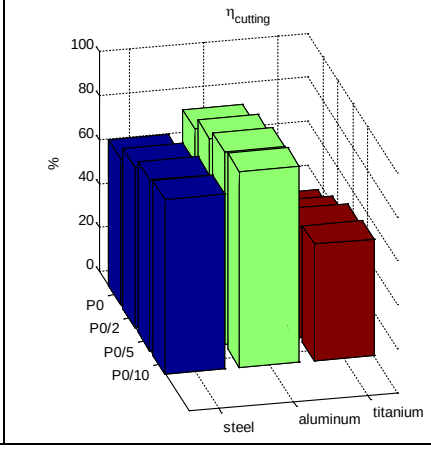	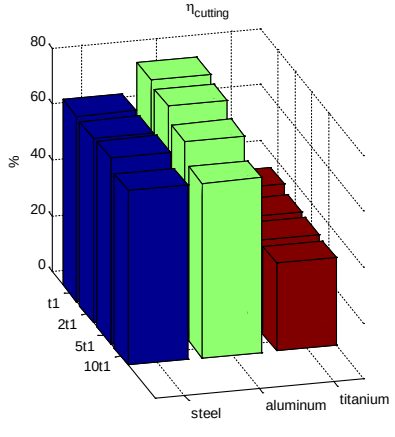

SE_{axes}/SE_{total} [%]	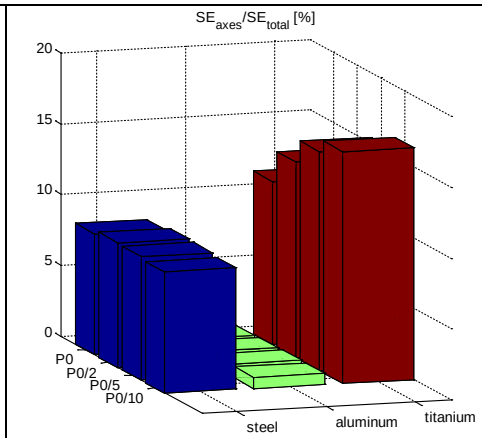	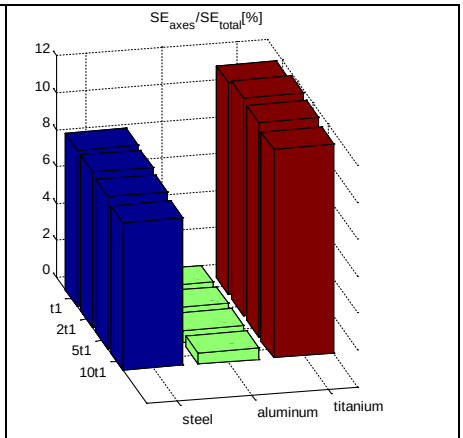
SE_{total}	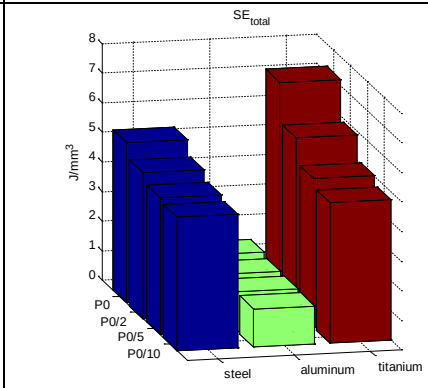	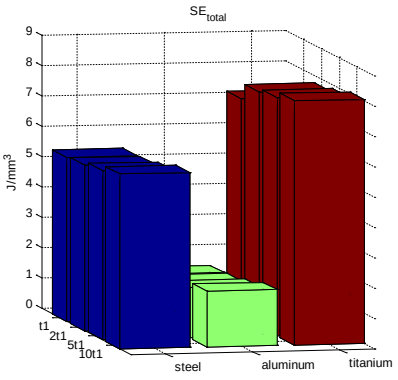
$1/MRR$	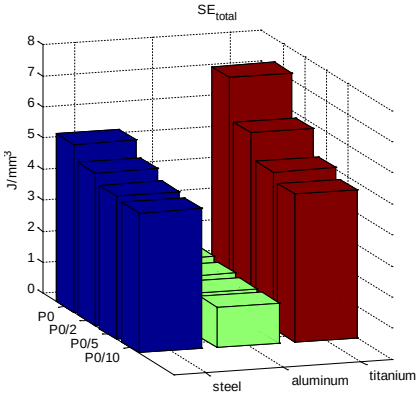	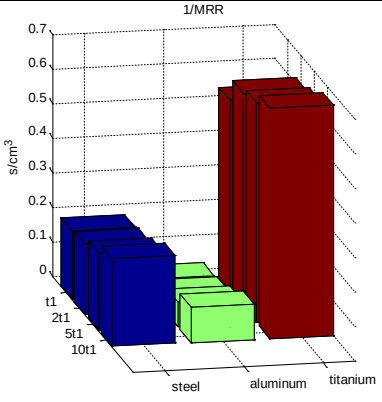
Optimal v_c The optimal energy conditions refer to $d_r = 80mm$ $f_z = 0.3mm/tooth$	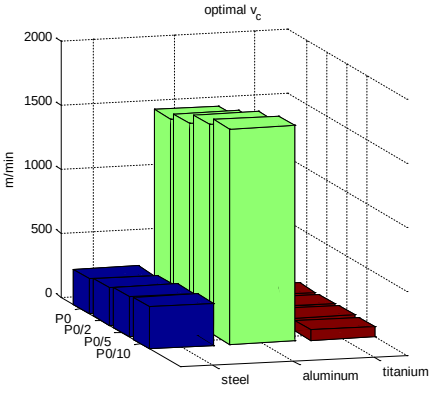	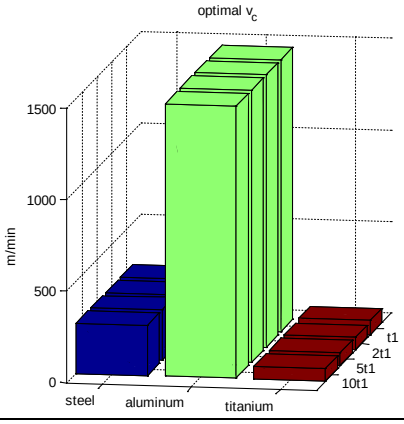

Fig. 12: sensitive analysis, simulation results

Note: Both appropriate cutting parameter ranges and Taylor's coefficients were considered according to the material to be processed.

6. Conclusions

In this paper, an analytical model able to estimate the machine tool energy consumption while processing a workpiece, was developed. The energy consumption in each individual machine functional module can be examined separately. A simplified machining strategy based on face milling operations (up/down milling) was modelled for evaluating the energy consumed during both machining and passive phases (tool change, workpiece preparation, etc). The wear of the tool wear was considered in the model through the Taylor's equation. Some of the parameters of the energy model were found through experimental tests performed on a machine center.

A multi-variable energy optimization was carried out considering the following process parameters(cutting speed, feed rate and radial depth of cut). The optimization was performed through a multi-dimensional exhaustive enumeration method. For each combination of feed and radial depth of cut, the optimized cutting velocity was found. It was observed that the cutting velocity that minimizes the global specific energy is slightly different from the velocity value that minimizes the specific production time. It was found that the same combination of axes feed and radial depth of cut allows minimizing the specific global energy and obtaining a quite low specific production time even if it is not the minimum achievable one. More in detail, the cutting condition corresponding to the minimum consumed energy is obtained setting both the parameters (radial depth of cut and feed) at their maximum allowable technological values, even if this implies the maximum axes load and the corresponding maximum energy consumption.

It was demonstrated that the proper cutting parameters selection can be an effective way for reducing both the consumed energy and the production time. The develop machine tool energy model was also used for performing several simulations aimed at emulating interesting scenarios. For instance, different machine tool configurations were reproduced changing the stand-by power consumption. This sensitive analysis was carried out in order to analyze the effects on energy oriented process parameters optimization in the next machine tool generation that surely will be equipped with eco-auxiliaries. Other simulations considering different workpiece set-up times were done in order to extend the validity of the obtained results for a specific production scenario. Since the developed energy model considers the properties of the machine tool and can be quite easily configured, it could be used to analyze, from the energy perspective, different machine tool layouts and design alternatives during the early machine conception. This would surely be the objective of further research studies.

7. Acknowledgment

The authors would thank Nicla Frigerio for the proof-reading

References

Albertelli, P., Bianchi, G., Bigliani, A., Borgia, S., Matta, A., Zanotti, E., 2011.Evaluation of the energy consumption in machine tool: a combined analytical-experimental approach, 13th International MITIP Conference, Trondheim, Norway.

Altintas Y., 2012. Manufacturing Automation. Cambridge University Press

Avram, O., Xirouchakis, P.,2011.Evaluating the use phase energy requirements of a machine tool system,Journal of Cleaner Production, 19 (6-7), 699–711.

Balogun, V.A., Mativenga, P.T., 2013. Modelling of direct energy requirements in mechanical machining processes, Journal of Cleaner Production, 41, pp. 179-186.

Behrendt, T., Zein, A., Min, S., 2012. Development of an energy consumption monitoring procedure for machine tools, CIRP Annals - Manufacturing Technology 61, 43-46.

Calvanese ML, Albertelli P., Matta A., Taisch M., 2013. Analysis of energy consumption in CNC machining centers and determination of optimal cutting conditions, 20th CIRP International Conference on Life Cycle Engineering, Singapore.

CUTPRO Guide, Manufacturing Automation Laboratory Inc., http://www.malinc.com/products/cutpro/.

Diaz, N., Choi, S., Helu, M., Chen, Y., Jayanathan, S., Yasui, Y., Kong, D., Pavanaskar, S., Dornfeld, D., 2010. Machine Tool Design and Operation Strategies for Green Manufacturing. Proceedings of 4th CIRP International Conference on High Performance Cutting.

Diaz, N., Helu, M., Jarvis, A, Tönissen, S., Dornfeld. D., Schlosser, R., 2009. Strategies for minimum energy operation for precision machining, The Proceedings of MTTRF Annual Meeting.

Diaz, N., Helu, M., Jayanathan, S., Chen, Y., Horvath, A., Dornfeld, D., 2010. Environmental analysis of milling machine tool use in various manufacturing environments. Sustainable Systems and Technology (ISSST), 2010 IEEE International Symposium on, 17-19 May.

Diaz, N., Redelsheimer, E., Dornfeld, D., 2011. Energy consumption characterization and reduction strategies for milling machine tool use. Glocalized Solutions for Sustainability in Manufacturing, 263-267.

Draganescu, F., Gheorghe, M., Doicin, C.V., 2003. Models of machine tool efficiency and specific consumed energy. Journal of Materials Processing Technology, 141, 9-15.

Gotze, U., Koriath, H.J., Kolesnikov, A., Lindner, R., Paetzold, J., 2012. Integrated methodology for the evaluation of the energy-and cost-effectiveness of machine tools. CIRP Journal of Manufacturing Science and Technology 5, 151-163.

Gutowski, T., Dahmus, J., Thiriez, A., 2006. Electrical Energy Requirements for Manufacturing Processes. 13th CIRP International Conference of Life Cycle Engineering, Lueven, May 31st – June 2nd.

Hanafi, I., Khamlichi, A., Cabrera, F.M., Almansa, E., Jabbouri, A., 2012. Optimization of cutting conditions for sustainable machining of PEEK-CF 30 using TiN tools. Journal of Cleaner Production 33, 1-9.

He, Y., Liu, F., Wu, T., Zhong, F.P., Peng, B., 2012. Analysis and estimation of energy consumption for numerical control machining. Proceedings of The Institution of Mechanical Engineers Part B-Journal of Engineering Manufacture 226 (B2), 255-266.

Hu, S., Liu, F., He, Y., Hu, T., 2012. An on-line approach for energy efficiency monitoring of machine tools. J. Clean. Prod. 27, 133-140.

Huang, H. and Ameta, G., 2014. Computational energy estimation tools for machining operations during preliminary design. International Journal of Sustainable Engineering 7(2), 130-143.

Kara, S., Li, W., 2011. Unit process energy consumption models for material removal processes, CIRP Annals - Manufacturing Technology 60, 37-40.

Li, J., Lu, Y., Zhao, H., Li, P., Yao, Y., 2014. Optimization of cutting parameters for energy saving, Int J Adv Manuf Technol. 70, 117-124.

Li, L., Yan, J., Xing, Z., 2013. Energy requirements evaluation of milling machines based on thermal equilibrium and empirical modelling. Journal of Cleaner Production 52, 113-121.

Li, W., Kara, S., 2011. An empirical model for predicting energy consumption of manufacturing processes: a case of turning process, Proc. Inst. Mech. Eng. Part B J. Eng. Manuf. 225 (B9), 1636-1646.

Mativenga, P.T., Rajemi, M.F., 2011. Calculation of optimum cutting parameters based on minimum energy footprint. CIRP Annals - Manufacturing Technology, 60, pp. 149-152.

Mori,M., Fujishima, M., Inamasu, Y., Oda, Y., 2011. A study on energy efficiency improvement for machine

tools. CIRP Annals - Manufacturing Technology 60, 145-148.

Newman, S.T., Nassehi, A., Imani-Asrai, R., Dhokia, V., 2012. Energy efficient process planning for CNC machining. CIRP J. Manuf. Sci.Technol. 5(2), 127-136.

Rajemi, M., Mativenga, P., Aramcharoen, A., 2010. Sustainable machining: selection of optimum turning conditions based on, Journal of Cleaner Production 18(10-11), 1059-1065.

Schmidt, C., Li, W., Thiede, S., Kara, S., Herrmann, C., 2015. A Methodology for customized Prediction of Energy Consumption in Manufacturing Industries. International Journal of Precision Engineering and Manufacturing-Green Technology, 2 (2), 163-172.

Thiede, S., Bogdanski, G., Herrmann, C., 2012. A Systematic Method for Increasing the Energy and Resource Efficiency in Manufacturing Companies, Procedia CIRP, Vol 2, 28-33.

Wang, Q., Liu F., Wang, X., 2014. Multi-objective optimization of machining parameters considering energy consumption, Int J Adv Manuf Technol 71, 1133-1142.

Yang, Y., Li, X., Gao, L., Shao, X., 2013. Modelling and impact factors analysing of energy consumption in CNC face milling using GRASP gene expression programming, Int J Adv Manuf Technol. doi:10.1007/s00170-013-5017-7.

Yingjie, Z., 2013. Energy efficiency techniques in machining process: a review. Int. J. Adv. Manuf. Technol., DOI 10.1007/s00170-013-5551-3.

Zhou, L., Li, J, Li, F., Meng, Q., Li, J., Xu, X., 2015. Energy Consumption Model and Energy Efficiency of Machine Tools: A Comprehensive Literature Review. Journal of Cleaner Production. http://dx.doi.org/10.1016/j.jclepro.2015.05.093.